Predictive performance of wildfire structure exposure modeling in the western US

Tyler J Hoecker*; tyler.hoecker@pyrologix.com; https://orcid.org/0000-0001-8680-8809

Matthew P Thompson; matt.thompson@pyrologix.com; https://orcid.org/0000-0002-2322-7756

Bryce A Young; bryce.young@pyrologix.com; https://orcid.org/0009-0000-1689-6065

Joe H Scott; joe.scott@pyrologix.com; https://orcid.org/0009-0008-3246-1190

Christopher J Moran; chris.moran@pyrologix.com; https://orcid.org/0000-0003-3378-8001

Kayleigh Wilson; kayleigh.wilson@pyrologix.com; https://orcid.org/0009-0000-2587-6779

Jeremy Arkin; jeremy.arkin@pyrologix.com; https://orcid.org/0000-0003-3373-5233

Michael Callahan; michael.callahan@pyrologix.com

Pyrologix, Vibrant Planet, Missoula, USA

*Corresponding author

Note: This paper is a non-peer reviewed preprint submitted to EarthArXiv; although the authors are planning to submit for peer review in the Journal of Pyrogeography.

Abstract

As development expands and extreme wildfire events worsen, people and property are increasingly exposed to wildfire hazards, necessitating comprehensive and accurate community and structure risk assessment tools. A variety of modeling frameworks and indices have been applied to support community wildfire planning, but few have been evaluated against subsequent fire events, which is a key gap for advancing the science and practice of risk management. Here we evaluate the performance of the Structure Exposure Score (SES) at predicting subsequent structure exposure. Specifically we analyze a SES layer current to 2017 landscape conditions and evaluate predictive performance over the western US across 2017-2022. We describe SES and evaluate its ability to discriminate wildfire-exposed from unexposed structures relative to a random classifier using an AUC-ROC approach. Results show that the mean SES value of exposed structures was 78.95% higher than unexposed structures. We report a mean per-fire AUC of 0.83, and an overall AUC of 0.76; the lower overall AUC is attributed to challenges predicting exposure from wildlands when events transition to urban conflagrations. Burn probability alone performed similarly to SES, suggesting it is sufficient where general exposure patterns are the focus, and SES more appropriate where the magnitude of exposure matters. Ember load was also an important predictor, especially on a per-fire basis (AUC = 0.76), consistent with the known role of ember transport in driving structure exposure in WUI fire environments. This work provides a foundational benchmark for future exposure prediction and assessment.

Keywords: Structure Exposure Score; burn probability; AUC-ROC; wildland-urban interface; decision support; community mitigation

Introduction

In the US, expanding human development in the wildland-urban interface coupled with the increasing prevalence of extreme wildfire events is exacerbating community exposure and loss, likely to worsen with climate change (Balch et al. 2024; Carlson et al. 2025a; Coop et al. 2022; Radeloff et al. 2018). Managing community wildfire risk requires analysis of hazard, exposure, and vulnerability, as well as understanding where responsibilities and opportunities align to manage these risk components (Calkin et al. 2014; Iglesias et al. 2022). Exposure analysis – our focus here – characterizes the spatial overlap of wildfire hazard metrics with resources and assets (Thompson et al. 2016a). It is used extensively to inform efforts ranging from national investment prioritization to local fuel treatment layout and community wildfire protection planning (Ager et al. 2019; Headwaters Economics 2025a; Kolden and Henson 2019).

In the community risk context, common exposure analysis approaches include pairing simulated fire likelihood, fire intensity, or fire perimeter maps with community polygon, building density, or building footprint maps (Ager et al. 2021; Alcasena et al. 2021; Argañaraz et al. 2017; Erni et al. 2024; Hawbaker et al. 2023; Jaffe et al. 2024; Kearns et al. 2022; Palaiologou et al. 2022; Parisien et al. 2019; Salis et al. 2023). Some approaches further combine fire likelihood and intensity metrics to provide a single measure of integrated hazard, which can support comprehensive and streamlined exposure analysis (Dillon 2023; Jaffe et al. 2024; Scott et al. 2012). Translating fire and structure data into a single actionable exposure metric therefore requires purposeful design choices relevant to planning contexts and management objectives

(Agueda et al. 2023; Dunn et al. 2020; McFayden et al. 2019; Nepal et al. 2022; Papathoma-Köhle et al. 2025; Thompson et al. 2013).

Empirical evaluation of predictive performance is essential to guide exposure metric design choices and improvements (Fields et al. 2026; Headwaters Economics 2025b). Relevant evaluation work in the US varies in terms of focus on hazard or exposure metrics, comparison to historical or future observation data, and spatial scale (Carlson et al. 2025b; Moran et al. 2025a; Ager et al. 2021, 2026). Building on this, here we present a novel exposure-focused evaluation effort comparing predictions based on 2017 landscape conditions against subsequent fire activity at the structure level, across the western US over the timeframe 2017-2022.

Specifically, we evaluate the predictive performance of Structure Exposure Score (SES), a relative index integrating fire likelihood and fire intensity (Scott et al. 2024). SES and its constituent data are publicly available in a variety of locations (Appendix A) and are used across a range of applications. Notable examples include home inspection prioritization by the California Department of Forestry and Fire Protection, project prioritization for community safety and ecological restoration through a Shared Stewardship agreement between the State of California and the USDA Forest Service Pacific Southwest Region, delineation of High Risk WUI areas by the Utah Division of Forestry, Fire, and State Lands, and dissemination of public risk information through various regional and state wildfire risk assessment portals. The widespread deployment of SES across these applications makes rigorous predictive evaluation practically important and timely.

Methods

SES Framework

The general equation of SES is [log-normalized likelihood] * [normalized intensity], with the full formulation outlined in Equations 1 and 2. Likelihood is quantified with annual Burn Probability (*BP*), derived using the large fire simulation system (FSim; Finney et al. 2011). Intensity is quantified with a composite metric termed Damage Potential (*DP*), derived using the Wildfire Exposure Simulation Tool (WildEST; Scott et al. 2024).

BP is log-scaled to account for a right-tailed distribution and to dampen the influence of *BP* relative to *DP*. A Normalization Constant (*NC)* is used to shift the floor of the log-transformed fire likelihood to a positive range. The current operational value of *NC* is set such that a *BP* of 1 in 100,000 results in a value of 1. Larger *BP* values yield a >1 multiplier for *DP*, and at the high end of *BP*, typically 1 in 10, the multiplier is ~10.

DP is a weighted combination of two dimensionless intensity metrics – Conditional Risk to Potential Structures (*cRPS*) and Conditional Ember Load Index (*cELI*) – and is capped at a value of 100. *cRPS* quantifies a relative measure of damage to structures based on flame length and lifeform (tree, shrub, or grass) without considering building features or materials. *cELI* quantifies the relative load of embers at a specific location, resulting from the combination of ember production and transport models that accumulate embers within grid cells downwind of the lofting cell. This formulation requires Weighting Factors (WF_1, WF_2) that determine the relative importance of one intensity variable versus the other, and a Scaling Factor (*SF*) that

adjusts the magnitude of *cELI* to match *cRPS*. In the current operational version, *cRPS* and *cELI* are assigned equal weights (0.5), and *SF* is set to 0.009 based on empirical calibration.

$$SES = [ln(BP) + NC] * DP \quad (1)$$

$$DP = min\left\{\left[WF_1 * cRPS + WF_2 * SF * cELI\right], 100\right\} \quad (2)$$

In recent years, the nomenclature has evolved where Wildfire Exposure Score (WES) is mapped broadly, reflecting potential exposure to any resource or asset, and SES is derived from WES through intersection with existing or planned structure footprints. Both layers extend beyond areas typically mapped as exposed to wildfire based on an index of burnable vegetation. This index is based on distance to patches of vegetative fuels with a minimum area of 500ha. Any burnable pixel has a value of 1, indicating the possibility of direct flame exposure to wildfire. Any non-burnable pixel has a value between 0 and 1 that decays with distance to large wildland patches, up to 2400m, indicating the possibility of indirect exposure via embers or structure-to-structure fire spread. 2400m is a calibrated value based on observed distances of structure loss from large wildland patches. Nonburnable pixels more than 2400m from large wildland patches have a value of 0, indicating a very low possibility of direct or indirect wildfire exposure. The intent of the burnable vegetation index is to mimic the decay of wildfire exposure into otherwise nonburnable developed areas. WES and SES are mapped everywhere the burnable vegetation index is greater than zero.

Exposure Analysis

We compared SES predictions to subsequent structure-level exposure observation data hosted by the US Geological Survey ScienceBase repository (Carlson et al. 2025a). This dataset covers the conterminous US over the timeframe 2002-2022, and catalogs buildings that were exposed to wildfires, for incidents where ≥10 buildings were destroyed. Regardless of damage status, our analysis included as “exposed” all buildings that were labeled as “directly exposed”, which includes buildings inside of or within 100m of mapped perimeters. We excluded that study’s “indirectly exposed” data, as it includes all buildings within a 2.4km radius of mapped perimeters given plausible ember transport distances but without definitive identification of actual exposure.

We used SES maps reflecting landscape conditions in 2017, including disturbances that occurred through December 2016. We defined our spatial extent as the western US, inclusive of the states Arizona, California, Colorado, Idaho, Montana, Nevada, New Mexico, Oregon, Washington, Utah, and Wyoming. We defined our observation period as 2017-2022, an approximate timeframe over which the static SES map remains relevant before disturbance and other changes may require a refresh.

To compare SES and its components between exposed and unexposed structures, we generated a representative sample of unexposed structures using building footprints from the Overture Maps Foundation (2026) and fire perimeters from the Carlson et al. (2025a) data archive. We employed a stratified random sampling scheme based on the burnable vegetation index, such that the distribution of the burnable vegetation index was nearly identical between exposed and unexposed structures. This ensured that data representing both outcomes were

drawn from locations with similar potential for direct (e.g., immediately adjacent to wildland fuel) and indirect (e.g., wildland ember transport) exposure to wildfire. We randomly sampled building footprints (n = the number of exposed structures) from areas outside fire perimeters for incidents with a start date between January 2017 and December 2022. We then attributed SES and its component metrics to exposed and unexposed structures based on raster values at building footprint centroids.

We evaluated the ability of SES and its constituent elements (BP, cRPS, cELI) to discriminate between exposed and unexposed structures using Receiver Operator Characteristic (ROC) curves. We framed this evaluation as a classification problem with a binary outcome of observed structure exposure to a wildfire. In this process, model specificity (true negative rate) and sensitivity (true positive rate) are calculated and plotted across the full range of each predictor to form a ROC curve from which the Area Under the Curve (AUC) is calculated. We constructed ROC curves and calculated the AUC on a per-fire basis by comparing SES values at exposed structures within individual fire perimeters to an equally sized sample of SES values at unexposed structures drawn from our global unexposed pool; we then calculated the mean per-fire AUC. We also calculated ROC curves and the AUC on an overall basis by comparing SES values at all exposed structures across all fires with the entire stratified unexposed structure pool. On the per-fire basis, each fire contributes equally to the AUC, whereas in the overall AUC, fire events with a larger number of exposed structures effectively contribute more. AUC is the probability that a randomly selected positive instance will be ranked higher by the predictor than a randomly selected negative instance and is equivalent to the Mann-Whitney U statistic. We compared predictors AUC's to a random classifier, which has an AUC of 0.5.

Results

In total across the 11 western states, 151,518 structures were directly exposed to wildfire between 2017 and 2022, of which 50,206 were damaged (33.18%). Interannual variability in fire activity and structure exposure is evident, as is asymmetry where a minority of events account for the majority of exposure (Appendix B). Across all events, the distribution of SES for exposed structures is shifted to the right of unexposed structures, with a longer right tail. The K-S test shows a significant difference between the SES distributions ($D = 0.401$, $p < 0.001$) of exposed and unexposed structures (Figure 1), which we attribute to SES accuracy. The mean SES value of exposed structures was 78.95% higher than the mean for unexposed structures. Of all exposed structures, 99.94% had a non-zero SES value, indicating SES consistently assigns non-zero exposure potential to structures that subsequently experienced wildfire.

SES and BP exhibited nearly equivalent overall predictive performance (overall AUC = 0.76 vs. 0.75), though BP indicated slightly stronger discriminative ability on a per-fire basis (mean per-fire AUC 0.80 vs 0.83; Table 1; Figure 2). The comparable performance of these two predictors suggests that fire likelihood is the dominant driver of structure exposure at the spatial and temporal scales evaluated here. cELI showed moderate predictive value (overall AUC = 0.69), but performed stronger on a per-fire basis (mean per-fire AUC = 0.76). cRPS showed the weakest performance among the fire environment predictors (AUC = 0.60), offering modest discrimination above the random classifier baseline.

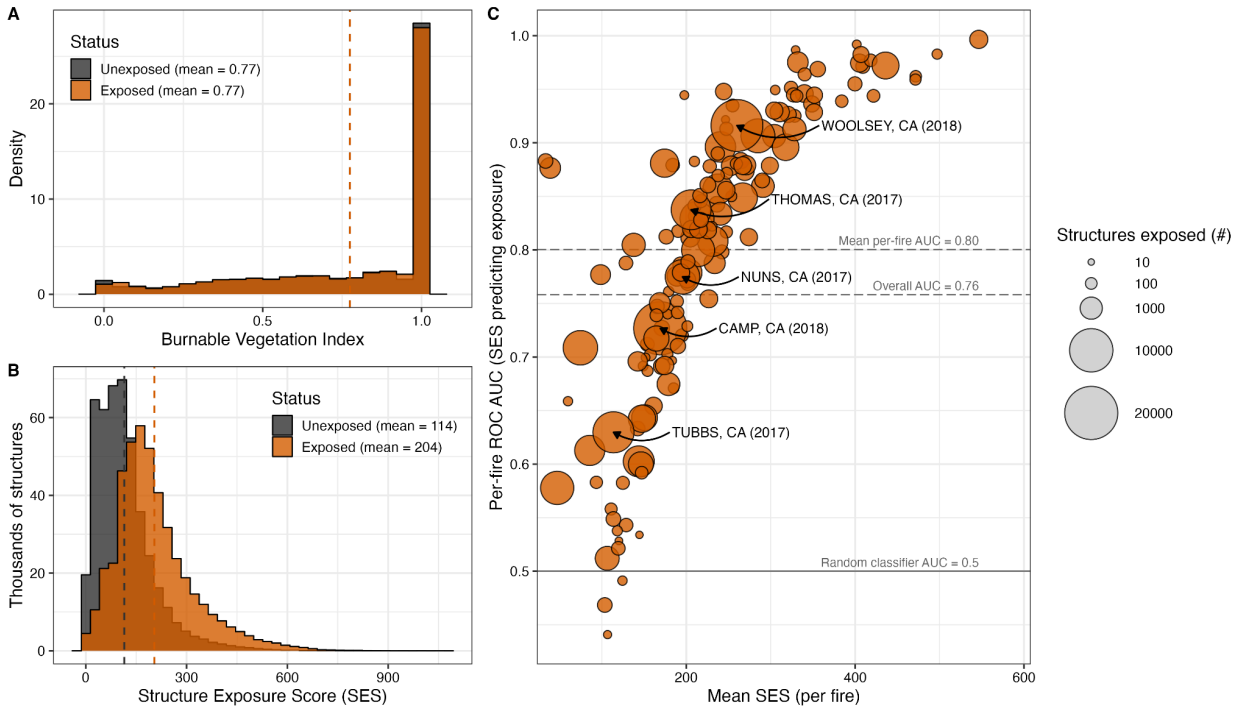

Figure 1. (A) Distributions of a burnable vegetation index used to stratify a random sample of unexposed (grey) structures. (B) the structure exposure scores of exposed (orange) and unexposed (grey) structures. Mean values for each set are shown. (C) Structure Exposure Score (SES) performance and mean fire-level SES for wildfires from 2017–2022. Each bubble represents one fire event. Bubble size is scaled to the number of exposed structures. The five events with the most structures exposed are labeled. Solid grey line marks the random-classifier baseline (AUC = 0.5); long-dashed reference lines indicate the mean per-fire AUC (0.80) and the overall AUC (0.76) computed across all exposed structures and a stratified sample of unexposed structures west-wide.

Table 1. Evaluation metrics for models predicting structure exposure. AUC is Area Under the Receiver-Operator Characteristic Curve.

Predictor	Overall AUC	Mean per-fire AUC
SES	0.76	0.80
BP	0.75	0.83
cELI	0.69	0.76
cRPS	0.60	0.64

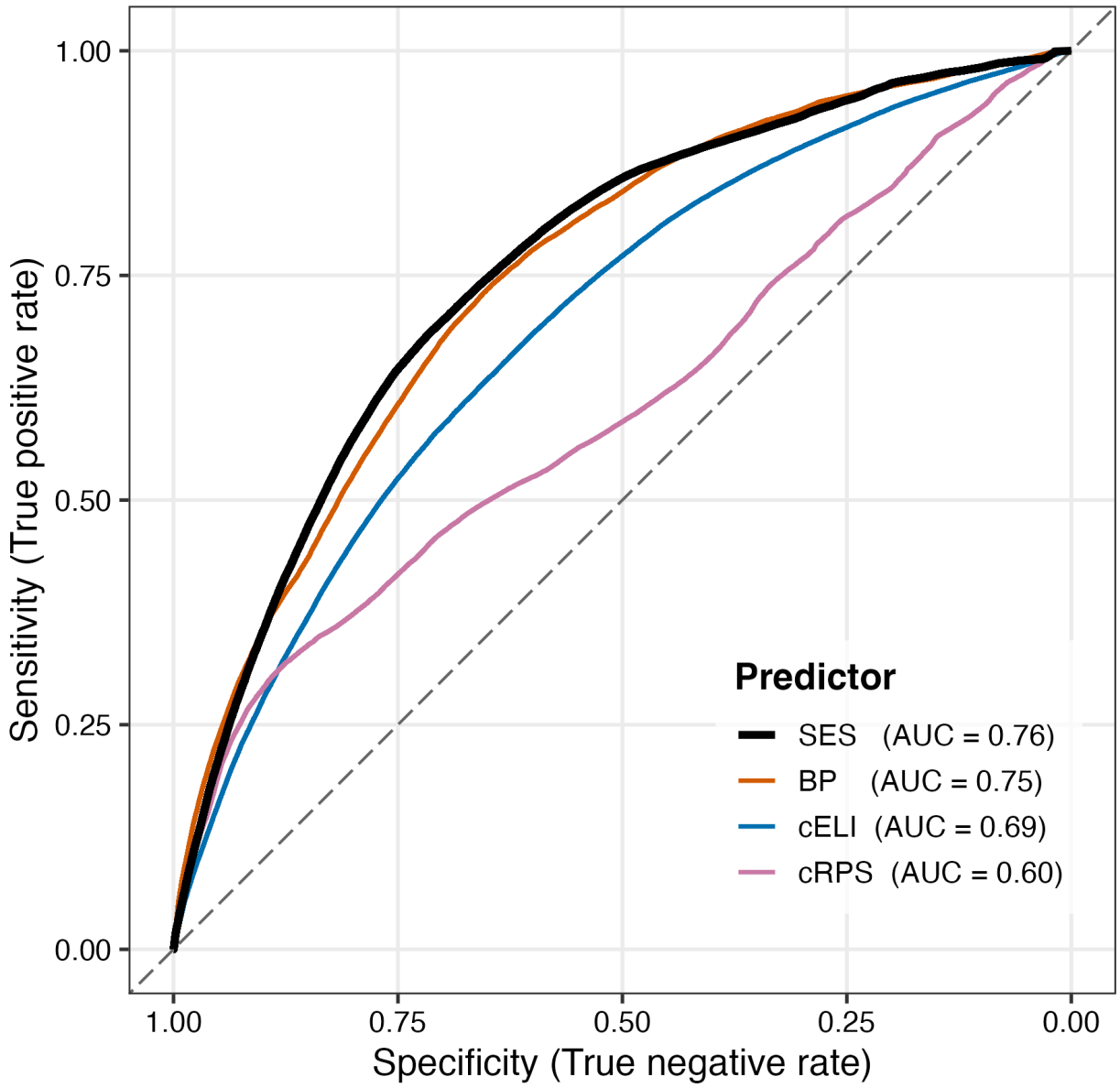

Figure 2. ROC curves for SES and its constituent elements for predicting structure exposure, across all fires.

Discussion

We found that exposed homes generally had higher SES values than unexposed structures (mean value 78.95% higher) even after controlling for proximity to burnable vegetation. The differences between exposed and unexposed structures reflect underlying differences in patterns of wildfire likelihood, intensity, and ember exposure, exactly what SES is designed to reveal. The overall AUC of 0.76 indicates that SES can correctly identify structures more likely to be exposed across diverse events and geographies. Relative to earlier work evaluating wildfire hazard and exposure models (Ager et al. 2021, 2026; Beverly and McLoughlin 2019;

Carlson et al. 2025a; Moran et al. 2025) this work is among the first evaluations of predicted exposure against subsequent fire activity at the level of individual structures.

The divergence between overall and per-fire performance is likely due to several high-exposure, high-loss urban conflagration events (e.g., the Tubbs Fire and the Camp Fire; Figure 1). In such events, we would expect lower SES values deeper into the built environment where fire spread is sustained through structure-to-structure ignitions. This result illustrates the limited ability of wildland-driven exposure models to capture urban-driven exposure mechanisms, and calls for clear articulation of what information SES does and does not provide. SES is not a structure loss model nor is it an urban exposure model. Where events are driven primarily by wildland exposure, the mean per-fire AUC of 0.80 indicates strong discriminative ability and many events exhibited AUC values greater than 0.9.

The focus on appropriate context and model translation for real-world use naturally leads to the question of when practitioners should use SES over BP. The comparable performance of BP and SES is notable, and indicates that the integrated hazard formulation of SES does not sacrifice predictive accuracy relative to fire likelihood alone. At the same time, this evaluation does not fully exercise the magnitude dimension that distinguishes SES from BP. Intensity and in particular ember load have direct relevance for mitigation planning given the well-known role of embers in structure exposure and ignition risk (Beverly et al. 2010; Caton et al. 2017; Manzello et al. 2020; Maranghides and Mell 2012). The per-fire performance of cELI (mean AUC = 0.76) indicates moderate discriminative ability for ember exposure and reveals potential stand-alone uses, e.g., for determining construction classes in the International WUI Code. The comparatively lower predictive value of cRPS could reflect the stronger signal of embers or redundancy with BP as a measure of direct flame contact.

Where understanding general exposure patterns is sufficient, BP is a suitable choice. Where the magnitude of exposure matters, e.g., for prioritizing defensible space inspections or determining codes, SES is more suitable. As one example of appropriate use, for managers and policymakers concerned about urban conflagration potential, the logical role for SES could be to identify highly exposed homes at the periphery of dense communities to target localized hardening. As another, for community protection planners, comparative scenario analysis with re-simulation of SES could help identify fuel treatment strategies most likely to reduce structure exposure via interrupted fire spread paths or reduced ember production.

Modeling improvements scale from incremental adjustments within the current framework to data improvements enabling SES reformulation to broader modeling ecosystem innovations. One near-term adjustment could be to increase the Weighting Factor for cELI as distance to burnable vegetation increases, where indirect exposure via ember transport is a more likely pathway. Using flame length metrics directly, rather than the loss functions embedded within cRPS, could also be explored. Better availability and quality of building footprint, building damage, and fire perimeter data open the door for SES to evolve into more empirically-driven and probabilistic formulations of structure exposure and loss.

More broadly, we anticipate that predictive performance and applicability will improve as more information about the built environment is incorporated into hazard, exposure, and vulnerability models (Fields et al. 2026). Deploying calibrated, customized fire behavior fuel models for

developed areas, which are often mapped as nonburnable, can better match observed rates of spread in the built environment (e.g., Moran et al. 2025b). Similarly, coupled wildland and urban models that account for structure-to-structure spread have shown promising results recreating significant historical events (e.g., Purnomo et al. 2024).

A number of limitations are worth noting. Our scope of inference is limited to the set of historical fires and geographies we considered; results may not hold against a different set of fires or time windows. Our use of point estimates for AUC may mask important variability within or across fire events, particularly for high-loss urban interface events. Our use of the Carlson et al. (2025a) dataset may bias the comparison data against smaller or less damaging fires that may have different primary exposure mechanisms, although it is the most comprehensive structure exposure dataset publicly available. It is important to clearly state that the authors of this manuscript were integrally involved in the design, modeling, and delivery of SES to clients; the methodology was designed to address this through use of independent external datasets, stratified sampling design, and comparison against baseline predictors.

Understanding risk at structure and community scales is an active area of interest, investment, and need. It requires coordination and collaboration across disciplines, innovations in fire science and engineering for model development, and transparent evaluation of model performance especially where deployed to guide mitigation plans (Headwaters Economics 2025c). Our main contribution here was predictive evaluation of a widely used structure exposure metric, providing a foundational benchmark for future exposure prediction and assessment.

Data Availability

The building footprint, fire perimeter, and structure exposure data are publicly available at the locations cited. The 2017 SES layer can be made available for research purposes upon reasonable request.

Declaration of Competing Interests

All co-authors either currently work for Vibrant Planet or worked for Vibrant Planet in the past.

Acknowledgments

The authors wish to thank the many fire scientists and practitioners who have helped improve the design and application of SES and its constituent layers over time. Specifically colleagues at the California Department of Forestry and Fire Protection, the Utah Department of Forestry, Fire, and State Lands, and the Missoula Fire Sciences Lab.

References

Ager AA, Day MA, Palaiologou P, Houtman RM, Ringo C, Evers CR (2019) Cross-boundary wildfire and community exposure: a framework and application in the Western US Gen. Tech. Rep. RMRSGTR-392. Forest Service US Department of Agriculture, Rocky Mountain Research Station, Fort Collins, CO.

Ager, A.A., Day, M.A., Alcasena, F.J., Evers, C.R., Short, K.C. and Grenfell, I., 2021. Predicting Paradise: Modeling future wildfire disasters in the western US. Science of the total environment, 784, p.147057.

Ager, A.A., Day, M.A., Evers, C.R., Kim, J.B., Kerns, B.K. and Ringo, C.D., 2026. Risk assessment in the Pyrocene–Rapid changes in models and predictions complicate US policies to prioritize forest and fuel management. Landscape and Urban Planning, 274, p.105695.

Argañaraz, J.P., Radeloff, V.C., Bar-Massada, A., Gavier-Pizarro, G.I., Scavuzzo, C.M. and Bellis, L.M., 2017. Assessing wildfire exposure in the Wildland-Urban Interface area of the mountains of central Argentina. Journal of environmental management, 196, pp.499-510.

Balch, J.K., Iglesias, V., Mahood, A.L., Cook, M.C., Amaral, C., DeCastro, A., Leyk, S., McIntosh, T.L., Nagy, R.C., St. Denis, L. and Tuff, T., 2024. The fastest-growing and most destructive fires in the US (2001 to 2020). Science, 386(6720), pp.425-431.

Beverly, J.L., Bothwell, P., Conner, J.C.R. and Herd, E.P.K., 2010. Assessing the exposure of the built environment to potential ignition sources generated from vegetative fuel. International journal of wildland fire, 19(3), pp.299-313.

Beverly, J.L. and McLoughlin, N., 2019. Burn probability simulation and subsequent wildland fire activity in Alberta, Canada–Implications for risk assessment and strategic planning. Forest Ecology and Management, 451, p.117490.

Calkin, D.E., Cohen, J.D., Finney, M.A. and Thompson, M.P., 2014. How risk management can prevent future wildfire disasters in the wildland-urban interface. Proceedings of the National Academy of Sciences, 111(2), pp.746-751.

Carlson, A.R., Hawbaker, T.J., Bair, L.S., Hoffman, C.M., Meldrum, J.R., Baggett, L.S. and Steblein, P.F., 2025a. Evaluating a simulation-based wildfire burn probability map for the conterminous US. International Journal of Wildland Fire, 34(1), p.WF23196.

Carlson, A.R., Hawbaker, T.J., Mockrin, M.H., Radeloff, V.C., Bair, L.S., Caggiano, M.D., Meldrum, J.R., Alexandre, P.M., Kramer, H.A. and Steblein, P.F., 2025b. Rising rates of wildfire building destruction in the conterminous United States. Proceedings of the National Academy of Sciences, 122(51), p.e2505886122.

Caton SE, Hakes RSP, Gorham DJ, Zhou A, Gollner MJ (2017) Review of pathways for building fire spread in the wildland-urban interface. Part I: exposure conditions. Fire Technology 53, 429-473.

Coop, J.D., Parks, S.A., Stevens-Rumann, C.S., Ritter, S.M. and Hoffman, C.M., 2022. Extreme fire spread events and area burned under recent and future climate in the western USA. Global Ecology and Biogeography, 31(10), pp.1949-1959.

El Ezz, A.A., Boucher, J., Cotton-Gagnon, A. and Godbout, A., 2022. Framework for spatial incident-level wildfire risk modelling to residential structures at the wildland urban interface. Fire safety journal, 131, p.103625.

Erni, S., Wang, X., Swystun, T., Taylor, S.W., Parisien, M.A., Robinne, F.N., Eddy, B., Oliver, J., Armitage, B. and Flannigan, M.D., 2024. Mapping wildfire hazard, vulnerability, and risk to Canadian communities. International journal of disaster risk reduction, 101, p.104221.

Finney, M.A., McHugh, C.W., Grenfell, I.C., Riley, K.L. and Short, K.C., 2011. A simulation of probabilistic wildfire risk components for the continental United States. Stochastic Environmental Research and Risk Assessment, 25(7), pp.973-1000.

Hawbaker, T.J., Henne, P.D., Vanderhoof, M.K., Carlson, A.R., Mockrin, M.H. and Radeloff, V.C., 2023. Changes in wildfire occurrence and risk to homes from 1990 through 2019 in the Southern Rocky Mountains, USA. Ecosphere, 14(2), p.e4403.

Headwaters Economics, 2025a. America's urban wildfire crisis: More than 1,100 communities at risk. Available at: https://headwaterseconomics.org/natural-hazards/wildfire/more-than-1100-communities-urban-wildfire-risk/

Headwaters Economics, 2025b. Wildfire Risk Indices & the Built Environment: Part 1 - An Inventory of Current Models. Available at: https://headwaterseconomics.org/wp-content/uploads/2025/08/2025-Wildfire-Risk-Indices-Part-1-Inventory-of-Existing-Models.pdf

Headwaters Economics, 2025c. Wildfire Risk Indices & the Built Environment: Part 2 - Gaps and Opportunities. Available at: https://headwaterseconomics.org/wp-content/uploads/2025/08/2025-Wildfire-Risk-Indices-Part-2-Gaps-and-Opportunities.pdf.

Iglesias, V., Stavros, N., Balch, J.K., Barrett, K., Cobian-Iñiguez, J., Hester, C., Kolden, C.A., Leyk, S., Nagy, R.C., Reid, C.E. and Wiedinmyer, C., 2022. Fires that matter: reconceptualizing fire risk to include interactions between humans and the natural environment. Environmental Research Letters, 17(4), p.045014.

Jaffe, Melissa R.; Scott, Joe H.; Callahan, Michael N.; Dillon, Gregory K.; Karau, Eva C.; Lazarz, Mitchell T. 2024. Wildfire Risk to Communities: Spatial datasets of wildfire risk for populated areas in the United States. 2nd Edition. Updated 10 September 2024. Fort Collins, CO: Forest Service Research Data Archive. https://doi.org/10.2737/RDS-2020-0060-2.

Kearns, E.J., Saah, D., Levine, C.R., Lautenberger, C., Doherty, O.M., Porter, J.R., Amodeo, M., Rudeen, C., Woodward, K.D., Johnson, G.W. and Markert, K., 2022. The construction of

probabilistic wildfire risk estimates for individual real estate parcels for the contiguous United States. Fire, 5(4), p.117.

Kolden, C.A. and Henson, C., 2019. A socio-ecological approach to mitigating wildfire vulnerability in the wildland urban interface: A case study from the 2017 Thomas fire. Fire, 2(1), p.9.

Manzello SL, Suzuki S, Gollner MJ, Fernandez-Pello AC (2020) Role of firebrand combustion in large outdoor fire spread. Prog Energy Combust Sci 76:100801.

Maranghides, A. and Mell, W., 2012. Framework for addressing the national wildland urban interface fire problem—determining fire and ember exposure zones using a WUI hazard scale. US Department of Commerce, National Institute of Standards and Technology. 25 p. doi:10.6028/NIST.TN.1748.

Moran, C.J., Thompson, M.P., Young, B.A., Scott, J.H. and Jaffe, M.R., 2025a. Benchmarking performance of annual burn probability modeling against subsequent wildfire activity in California. Scientific Reports, 15(1), p.23699.

Moran, C.J., Seielstad, C.A. and Pietruszka, B.M., 2025b. Three fuel models for predicting urban fire spread–a stopgap for emergency management in the US. International Journal of Wildland Fire, 34(11), p.WF24132.

Overture Maps Foundation, overturemaps.org. Release date 5/20/2026.

Parisien, M.A., Dawe, D.A., Miller, C., Stockdale, C.A. and Armitage, O.B., 2019. Applications of simulation-based burn probability modelling: a review. International journal of wildland fire, 28(12), pp.913-926.

Purnomo, D.M., Qin, Y., Theodori, M., Zamanialaei, M., Lautenberger, C., Trouvé, A. and Gollner, M.J., 2024. Integrating an urban fire model into an operational wildland fire model to simulate one dimensional wildland–urban interface fires: a parametric study. International Journal of Wildland Fire, 33(10), p.WF24102.

Radeloff, V.C., Helmers, D.P., Kramer, H.A., Mockrin, M.H., Alexandre, P.M., Bar-Massada, A., Butsic, V., Hawbaker, T.J., Martinuzzi, S., Syphard, A.D. and Stewart, S.I., 2018. Rapid growth of the US wildland-urban interface raises wildfire risk. Proceedings of the national academy of sciences, 115(13), pp.3314-3319.

Salis, M., Del Giudice, L., Alcasena-Urdiroz, F., Jahdi, R., Arca, B., Pellizzaro, G., Scarpa, C. and Duce, P., 2023. Assessing cross-boundary wildfire hazard, transmission, and exposure to communities in the Italy-France Maritime cooperation area. Frontiers in Forests and Global Change, 6, p.1241378.

Scott, J., Helmbrecht, D., Thompson, M.P., Calkin, D.E. and Marcille, K., 2012. Probabilistic assessment of wildfire hazard and municipal watershed exposure. Natural Hazards, 64(1), pp.707-728.

Joe H. Scott, Christopher Moran, Michael Callahan, April Brough, Matthew P Thompson. 2024. WildEST—the Wildfire Exposure Simulation Tool. doi: 10.17605/OSF.IO/VEDKC. Available at: https://osf.io/vedkc/overview. (Accessed 1 April 2026).

Thompson, M.P., Zimmerman, T., Mindar, D. and Taber, M., 2016. Risk terminology primer: basic principles and a glossary for the wildland fire management community. Gen. Tech. Rep. RMRS-GTR-349. Fort Collins, CO: US Department of Agriculture, Forest Service, Rocky Mountain Research Station. 13 p., 349.

Appendix A

Table A.1: Non-exhaustive list of publicly available sources of structure exposure score (SES) and related or constituent data. BP = burn probability. DP = damage potential. cELI = conditional ember load index; cRPS = conditional risk to potential structures; ELI = ember load index (BP * cELI); RPS = risk to potential structures (BP * cRPS); WES = wildfire exposure score.

Description	Layers	URL
California Regional Resource Kits	BP, DP, DP, ELI, **SES**	https://caregionalresourcekits.org/
CAL FIRE Hazard and Risk Data	BP, cELI, cRPS, DP, **SES**	https://www.vpdatacommons.org/datasets/cal-fire-wildfire-hazard-risk-modeling-2020-2035
Northeast-Midwest Wildfire Risk Explorer	BP, cRPS, RPS	https://wrap.northeastmidwestwildfirerisk.com/Map/Public/
Nevada Natural Resources and Fire Information Portal	BP, cRPS, ELI, RPS	https://wrap.nevadaresourcesandwildfireinfo.com/Map/Public/#map-themes
Southern Wildfire Risk Explorer	BP, DP, **WES**	https://wrap.southernwildfirerisk.com/Map/Public/
Texas Wildfire Risk Explorer	BP, DP, **WES**	https://wrap.texaswildfirerisk.com/Map/Public/
Utah Wildfire Risk Explorer	BP, DP, **SES**	https://wrap.wildfirerisk.utah.gov/Map/Public/
Wildfire Risk to Communities	BP, cRPS, RPS	https://wildfirerisk.org/download/

Appendix B

Table B.1. Summary of all observed structure exposure including high exposure events.

Fire	State	Mean SES	Exposed	Damaged
2017				
All fires		177	34,289	9,913
TUBBS	CA	114	8,314	5,185
THOMAS	CA	206	7,503	956
NUNS	CA	196	4,596	1,023
2018				
All fires		226	50,312	21,029
CAMP	CA	169	21,333	16,486
WOOLSEY	CA	260	18,414	1,508
CARR	CA	285	4,334	1,677
2019				
All fires		173	4,015	374
TICK	CA	174	2,315	29
KINCADE	CA	165	1,559	272
SANDALWOOD	CA	255	141	73
2020				
All fires		194	45,082	13,776
BEACHIE CREEK	OR	75	4,594	856
GLASS	CA	213	4,377	1,237
ALMEDA DRIVE	OR	47	4,034	2,396
2021				
All fires		207	14,505	4,293
DIXIE	CA	231	3,011	1,029
MARSHALL	CO	86	2,882	1,187
CALDOR	CA	267	2,680	943
2022				
All fires		310	3,315	891
OAK	CA	253	627	181
MCBRIDE	NM	546	496	159
TUNNEL	AZ	304	405	48